Available online at www.sciencedirect.com
SCIENCE DIRECT®
ELSEVIER
Earth and Planetary Science Letters 216 (2003) 313–328
EPSL
www.elsevier.com/locate/epsl

The structure and sharpness of $(Mg,Fe)_2SiO_4$ phase transformations in the transition zone☆

Daniel J. Frost *

Bayerisches Geoinstitut, Universität Bayreuth, D-95440 Bayreuth, Germany

Received 28 February 2003; received in revised form 4 July 2003; accepted 19 September 2003

Abstract

To calculate accurately the pressure interval and mineral proportions (i.e. yields) across the olivine to wadsleyite and wadsleyite to ringwoodite transformations requires a detailed knowledge of the non-ideality of Fe–Mg mixing in these $(Mg,Fe)_2SiO_4$ solid solutions. In order to constrain the activity–composition relations that describe non-ideal mixing, Fe–Mg partitioning experiments have been conducted between magnesiowüstite and $(Mg,Fe)_2SiO_4$ olivine, wadsleyite and ringwoodite as a function of pressure at 1400°C. Using known activity–composition relations for magnesiowüstite the corresponding relations for the three polymorphs were determined from the partitioning data. In all experiments the presence of metallic iron ensured redox conditions compatible with the Earth's transition zone. The non-ideality of the $(Mg,Fe)_2SiO_4$ solid solutions was found to decrease in the order $W_{FeMg}^{wadsleyite} > W_{FeMg}^{ringwoodite} > W_{FeMg}^{olivine}$. These partitioning data were used, along with published phase equilibria measurements for the Mg_2SiO_4 and Fe_2SiO_4 end-member transformations, to produce an internally consistent thermodynamic model for the Mg_2SiO_4–Fe_2SiO_4 system at 1400°C. Using this model the pressure interval of the olivine to wadsleyite transformation is calculated to be significantly smaller than previous determinations. By combining these results with Fe–Mg partitioning data for garnet, the widths of transition zone phase transformations in a peridotite composition were calculated. The olivine to wadsleyite transformation at 1400°C in dry peridotite was found to occur over a pressure interval equivalent to approximately 6 km depth and the mineral yields were found to vary almost linearly with depth across the transformation. This transformation is likely to be even sharper at higher temperatures or could be significantly broader in wet mantle or in regions with a significant vertical component of mantle flow. The entire range of estimated widths for the 410 km discontinuity (4–35 km) could, therefore, be explained by the olivine to wadsleyite transformation in a peridotite composition over a range of quite plausible mantle temperatures and H_2O contents. The wadsleyite to ringwoodite transformation in peridotite mantle was calculated to take place over an interval of 20 km at 1400°C. This transformation yield was also found to be near linear.

Keywords: wadsleyite; olivine; transition zone; element partitioning; oxygen fugacity; seismic discontinuity; 410 km discontinuity

* Tel.: +49-921-553737; Fax: +49-921-553769. *E-mail address:* dan.frost@uni-bayreuth.de (D.J. Frost).

☆ Supplementary data associated with this article can be found at doi:10.1016/S0012-821X(03)00533-8

0012-821X/03/$ – see front matter © 2003 Elsevier B.V. All rights reserved.
doi:10.1016/S0012-821X(03)00533-8

1. Introduction

The 410, 520 and 660 km seismic discontinuities (hereafter referred to as *d*410, *d*520 and *d*660) provide some of the only clues as to the physical and chemical state of the mantle in the transition zone. The depth, width and amplitude of these discontinuities will depend on the mantle temperature, chemical composition and mineral proportions [1,2]. Several studies have identified significant topography of discontinuities in the transition zone [3,4], which might result from lateral variations in temperature. Similarly, recent studies have identified that *d*410 varies significantly in thickness in different parts of the mantle [5,6]. As more detailed seismic coverage of the mantle emerges it seems possible that an integrated model for the phase relations and elastic properties of mantle materials might eventually be used to invert seismic data to give a precise picture of the regional chemical composition and temperature in the transition zone. At present, however, many of the influences that may affect the position and width of transformations in the transition zone are quite poorly constrained.

Although it is now generally accepted that *d*410 is caused by the olivine to wadsleyite transformation, there are still a number of outstanding differences between seismic and experimental observations. Seismic observations of the width of *d*410, for example, show it to be quite sharp in some regions of the mantle with several estimates below 6 km [7–9]. Phase equilibrium determinations of the olivine to wadsleyite transformation in the Mg_2SiO_4–Fe_2SiO_4 system, however, yield a depth interval of over 10 km for typical mantle temperatures and compositions [10,11]. It has been proposed that a non-linear gradient in elastic properties across the olivine to wadsleyite transformation might sharpen the seismically observed discontinuity [12,13] and that Fe–Mg partitioning involving non-transforming phases, such as garnet, might have a similar effect [12,14]. There are very few precise experimental data available, however, with which to test these possibilities. On the other hand, components such as H_2O and Fe^{3+} might act to broaden the transformation interval of the olivine to wadsleyite transition [15–17]. These components might not only explain relatively broad *d*410 observations in some regions of the mantle [5,6,18] but because these components are often present, but go undetected in high-pressure experiments, their occurrence may have inadvertently broadened previous experimental determinations of the transformation interval. It is therefore important to first determine the phase relations of the Mg_2SiO_4–Fe_2SiO_4 system in the absence of H_2O and Fe^{3+} and then examine the effects when these components are added.

If the transformation of olivine to wadsleyite really can occur over a depth interval of less than 6 km then this corresponds to a transformation pressure interval of less than 2 kbar. This level of precision in pressure measurement is, however, very difficult to achieve in a multianvil phase equilibrium experiment at these conditions. Calorimetric measurements combined with mineral elasticity data are also not of sufficient accuracy to well constrain this transformation interval when used in isolation. The width of the olivine to wadsleyite transformation in the Mg_2SiO_4–Fe_2SiO_4 system, however, can be quite accurately calculated using knowledge of the thermodynamics of the Fe–Mg partitioning between the solid solutions involved and combining this with accurate phase equilibrium determinations only for the end-member Mg_2SiO_4 and Fe_2SiO_4 mineral transformations. In order to calculate the basic phase relations in the Mg_2SiO_4–Fe_2SiO_4 system I have performed a series of experiments to measure Fe–Mg partitioning between magnesiowüstite and the $(Mg,Fe)_2SiO_4$ polymorphs at 1400°C over a wide range of pressure. These partitioning relations do not vary strongly with pressure and can be used to refine thermodynamic data for the Mg_2SiO_4–Fe_2SiO_4 system that can be used to calculate accurate phase transformation pressure intervals [19]. These experiments were performed in equilibrium with metallic Fe to buffer Fe^{3+} concentrations at the lowest level. Analyses of mantle xenoliths indicate that the upper mantle has a relatively low $Fe^{3+}/\Sigma Fe$ ratio of approximately 2% [20]. Experiments have shown, however, that wadsleyite in equilibrium with metallic Fe has an $Fe^{3+}/\Sigma Fe$ ratio very similar to this upper mantle

ratio [20]. If the $Fe^{3+}/\Sigma Fe$ ratio of the upper mantle is the same as the transition zone, then the oxygen fugacity in this region will consequently be very close to metallic Fe saturation.

These results and the optimised thermodynamic data are used to calculate the pressure intervals of the olivine to wadsleyite and wadsleyite to ringwoodite transformations in peridotite mantle. The variety of factors and conditions that may result in locally sharp or broad discontinuities are then discussed.

2. Theoretical background

For a binary Mg_2SiO_4–Fe_2SiO_4 phase transformation the shape of the coexisting two-phase region is a function of the non-ideality of Fe–Mg mixing in each solid solution. The degree of non-ideality is described by the Fe–Mg activity–composition relationship, which can be determined through Fe–Mg partitioning experiments between a corresponding phase, in this case magnesiowüstite, for which these relations are already known.

The partitioning of iron and magnesium between olivine and magnesiowüstite can be described on a single site basis by the exchange reaction:

$$\underset{\text{magnesiowüstite}}{FeO} + \underset{\text{olivine}}{MgSi_{1/2}O_2} = \underset{\text{magnesiowüstite}}{MgO} + \underset{\text{olivine}}{FeSi_{1/2}O_2} \quad (1)$$

The equilibrium distribution coefficient K_D for this reaction is defined as:

$$K_D = \frac{X^{Mw}_{Mg} X^{Ol}_{Fe}}{X^{Ol}_{Mg} X^{Mw}_{Fe}} \quad (2)$$

where X^{Ol}_{Fe} is the molar Fe/(Fe+Mg) ratio. At equilibrium and at a fixed pressure and temperature the standard state Gibbs free energy change for exchange reaction (Eq. 1) is:

$$\Delta G^0_{(1)} = -RT\ln\frac{a^{Mw}_{Mg} a^{Ol}_{Fe}}{a^{Ol}_{Mg} a^{Mw}_{Fe}} \quad (3)$$

The activity–composition relationship is:

$$a^{Ol}_{Fe} = (X^{Ol}_{Fe} \cdot \gamma^{Ol}_{Fe}) \quad (4a)$$

$$a^{Ol}_{Mg} = (X^{Ol}_{Mg} \cdot \gamma^{Ol}_{Mg}) \quad (4b)$$

where γ^{Ol}_{Fe} is an activity coefficient, which describes the non-ideality of mixing. Identical formalisms can be written for magnesiowüstite. Eq. 3 can then be written as:

$$\Delta G^0_{(1)} = -RT\ln K_D - RT\ln\frac{\gamma^{Mw}_{Mg}\gamma^{Ol}_{Fe}}{\gamma^{Ol}_{Mg}\gamma^{Mw}_{Fe}} \quad (5)$$

The activity coefficients are also a function of composition. The simplest description for this variation is a so-called symmetric solution model, i.e.:

$$RT\ln\gamma^{Ol}_{Fe} = W^{Ol}_{FeMg}\left(1-X^{Ol}_{Fe}\right)^2 \quad (6a)$$

$$RT\ln\gamma^{Ol}_{Mg} = W^{Ol}_{FeMg}\left(1-X^{Ol}_{Mg}\right)^2 \quad (6b)$$

W^{Ol}_{FeMg} is a Margules interaction parameter where the magnitude of W equates to the degree of non-ideality of mixing. Two similar equations can be written to describe the activity coefficients of magnesiowüstite. For Fe–Mg mixing in most silicates W_{FeMg} is relatively small and a symmetric model is usually adequate to describe most data [16,21–23].

By using two symmetric interaction parameters to describe both solid solutions Eq. 3 can be rearranged to become:

$$\Delta G^0_{(1)} = -RT\ln K_D + W^{Ol}_{FeMg}\left(2X^{Ol}_{Fe}-1\right) + W^{Mw}_{FeMg}\left(1-2X^{Mw}_{Fe}\right) \quad (7)$$

Previous studies have shown that the application of Eq. 7 to experimental partitioning data collected over a range of Fe contents can provide good estimates for the difference between the two interaction parameters [21,24], but the individual parameters are highly correlated with each other. In order to refine one of the interaction parameters the other one must first be known. In several recent studies the activity composition relations for magnesiowüstite as a function of temperature and pressure have been extensively studied and the interaction parameter for this phase is now known very well [21,23,25]. I have performed experiments to measure the Fe–Mg partitioning be-

tween magnesiowüstite and olivine, wadsleyite and ringwoodite and used the previously determined interaction parameter for magnesiowüstite to determine this parameter for these polymorphs. A major benefit of using magnesiowüstite to determine activity–composition relations is that it coexists with all three $(Mg,Fe)_2SiO_4$ polymorphs over large ranges of pressure and composition. Whereas the $(Mg,Fe)_2SiO_4$ polymorphs themselves only coexist with each other at a single composition at a particular pressure and temperature. In this study $\Delta G^0_{(1)}$, the Gibbs free energy change of the ion exchange reaction (Eq. 1) at pressure and temperature is also used as a constraint in the refinement of internally consistent thermodynamic data for the high-pressure Mg_2SiO_4 and Fe_2SiO_4 end-member phases. Estimates of the Gibbs free energy change over a range of pressures provides much needed constraints on the magnitude of the volume change of the ion exchange reaction at pressure and temperature. These refined thermodynamic data are then used to calculate phase diagrams at high pressure in this system.

The interaction parameters also vary as a function of pressure and temperature according to:

$$W = W_U - TW_S + PW_V \quad (8)$$

In this study all data were collected at a single temperature so W_S is not considered. Values of W_V can be determined from the excess volumes of mixing, which for the olivine, magnesiowüstite and ringwoodite solid solutions are estimated to be 0.01, 0.011 and zero J/bar respectively [21,26,27] on a single site basis. The excess volume of mixing for the wadsleyite solid solution cannot be determined because the Fe_2SiO_4 end-member does not exist. As wadsleyite is stable over a narrow range of pressure, however, W_V can be quite reasonably assumed to be zero.

3. Experimental technique

Magnesiowüstite and olivine solid solutions of varying Fe/(Fe+Mg) ratio were prepared from reagent grade Fe_2O_3, MgO, and SiO_2. Ground mixtures of the required compositions were pressed into pellets and reduced in a gas mixing CO–CO_2 furnace between 1200 and 1300°C at an fO_2 1 log unit above the iron–wüstite oxygen buffer. Recovered samples were then reground and reduced a second time. Olivine and magnesiowüstite solid solutions in the molar ratio of 2:1 were then ground together with an additional 20 wt% metallic Fe to produce the starting compositions shown in Table 1. Compositions of both solid solutions were chosen such that they would approach the suspected equilibrium composition from both higher and lower initial Fe contents.

Experiments were performed in a split cylinder multianvil press using 10/5 (octahedral edge length/truncation edge length) and 18/11 octahedral sample assemblies and 32 mm Toshiba tungsten carbide cubes. Pressure calibrations for these assemblies have been previously reported [16]. Four-bore Al_2O_3 thermocouple ceramic rods were used as capsules. Two 0.5 mm long capsules were placed inside an outer molybdenum foil capsule with 0.2 mm thick Al_2O_3 discs between and at each end of the capsules. Powders were packed into the holes in each of the rods making a total of eight samples. After the experiment these capsules were cut in half along the disc that separated the two ceramic rods and both exposed sides were

Table 1
Starting compositions

	$(Mg,Fe)_2SiO_4$ Fe/(Fe+Mg)	(Mg,Fe)O Fe/(Fe+Mg)	K_D
AB	0.000	0.060	0.000
AC	0.050	0.000	∞
A	0.050	0.060	0.825
B	0.050	0.150	0.298
C	0.100	0.060	1.741
D	0.100	0.360	0.198
E	0.150	0.150	1.000
F	0.150	0.360	0.314
G	0.200	0.150	1.417
A2	0.000	0.200	0.000
B2	0.100	0.400	0.167
C2	0.200	0.100	2.250
D2	0.200	0.600	0.167
E2	0.400	0.400	1.000
F2	0.400	0.800	0.167
G2	0.600	0.600	1.000
H2	0.800	0.800	1.000
I2	0.600	0.800	0.375

Table 2
Experimental run conditions

Run	Assembly	Pressure (GPa)	Temperature (°C)	Time (hours)	Capsule	Phases observed (+mw)
PC1	0.5 inch	2.0	1400	24	graphite	olivine
V189	10/5	13	1400	26	$2\times Al_2O_3$	olivine/AnB
V191	10/5	14.5	1400	23	$2\times Al_2O_3$	wadsleyite
V192	10/5	9.0	1400	24	$2\times Al_2O_3$	olivine
V200	18/11	6.0	1400	100	$2\times Al_2O_3$	olivine
V208	18/11	11.0	1400	50	$2\times Al_2O_3$	olivine/ring
V209	10/5	14.0	1400	50	$2\times Al_2O_3$	olivine/wad/AnB
V212	10/5	16.0	1400	75	$2\times Al_2O_3$	wad/ring
V217	10/5	14.0	1400	26	$2\times Al_2O_3$	olivine/ring
V220	10/5	14.0	1400	24	$1\times Al_2O_3$	olivine/wad
V223	10/5	13.2	1400	24	$1\times Al_2O_3$	olivine/wad/ring
V227	10/5	13.0	1400	24	$1\times Al_2O_3$	olivine/wad/ring
V229	10/5	12.8	1400	29	$1\times Al_2O_3$	olivine/wad/ring
V252	10/5	12.4	1400	24	$1\times Al_2O_3$	olivine
V254	10/5	12.5	1400	29	$1\times Al_2O_3$	olivine/wad/ring

PC1 was performed in a piston cylinder. AnB is short for anhydrous phase B, wad is wadsleyite, ring is ringwoodite and mw is magnesiowüstite. See text for assembly and capsule details.

polished to reveal the eight sample chambers. The uncertainty in the temperature at the mid point of the two capsules is considered to be approximately 40°. In experiments performed to find the olivine–wadsleyite–ringwoodite 'triple point' a single capsule was used and the sample was sectioned and polished on the surface that was only separated from the thermocouple by a 0.2 mm thick Al_2O_3 disc, such that thermal gradients between the sample and thermocouple would have been negligible. All experimental conditions are given in Table 2. The phases present in the recovered charges were identified using Raman spectroscopy and an electron microprobe was used to analyse phase compositions.

4. Results

Experimental run products are reported in table 3[1] (on-line database). After all experiments metallic Fe remained dispersed through the sample and a very small rim (<20 μm) of garnet formed at the wall of the Al_2O_3 capsule. Between 12 and 14 GPa olivine reacted with magnesiowüstite to produce anhydrous phase B ($\{Mg,Fe\}_{14}Si_5O_{24}$).

Fig. 1a shows $RT\ln(K_D)$ for olivine–magnesiowüstite experiments performed between 2 and 13 GPa at 1400°C. The final compositions were approached from starting materials with initial values of K_D that were both higher and lower. Apart from some olivine compositions with Fe/(Fe+Mg) <0.05 the various compositions could be observed to reach equilibrium from both directions. In some cases both silicate and oxide increased in Fe/(Fe+Mg) ratio due to the oxidation of metallic Fe. K_D for this exchange reaction decreases slightly with pressure. Uncertainties in Fig. 1a are calculated from the 1σ standard deviation of the microprobe analyses.

The results of least squares fitting of these data using Eq. 7 with the known activity composition relations for magnesiowüstite ($W_U = 11\,100$ kJ, $W_V = 0.011$ J/bar [21]) are shown at 6 and 13 GPa. Using molar volume data to constrain W_V (0.01 J/bar) results in a refined value for W_U of 2 ± 1 kJ for the olivine solid solution. Values for $\Delta G^0_{(1)}$ obtained are -21.9 kJ at 6 GPa and -22.5 kJ at 13 GPa. Previous studies have shown that at 1 bar the $Fe^{3+}/\Sigma Fe$ ratio of magnesiowüstite in equilibrium with metallic Fe increases with Fe/(Fe+Mg) ratio to a maximum of approximately

[1] See online version of this article.

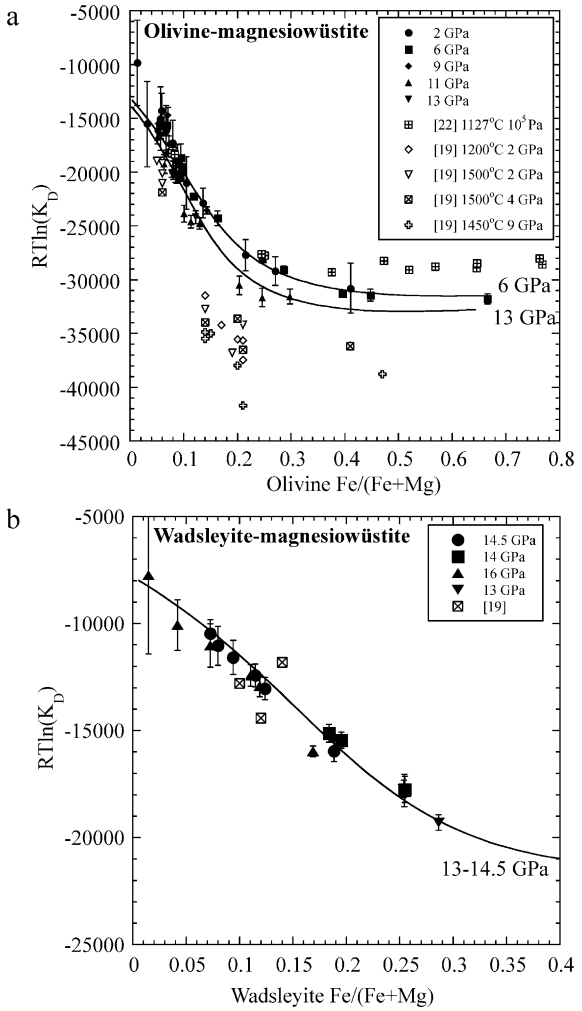

Fig. 1. Fe–Mg partitioning results for olivine–magnesiowüstite (a) and wadsleyite–magnesiowüstite (b) from experiments performed at 1400°C. K_D is defined as in Eq. 2 and the units of $RT\ln(K_D)$ are joules. A least squares fit of Eq. 7, using known activity–composition relations for magnesiowüstite, is shown at 6 and 13 GPa for olivine and for all data between 13 and 14.5 GPa for wadsleyite. The previous experimental results of Wiser and Wood [22] and Fei et al. [19] are shown for comparison.

10.5% in wüstite [23,25]. As the ferric iron content decreases with pressure [28], however, it is likely to be low in most of the samples studied here and has been ignored in the thermodynamic treatment. Only at 2 GPa is the ferric iron content of magnesiowüstite likely to be significant, which may explain why the partitioning data at 2 GPa are slightly lower than expected when compared to the 6 GPa data. The lower values of K_D reported by Fei et al. [19] might also have resulted from a slightly higher magnesiowüstite ferric iron content because molybdenum capsules were used. The experiments of Wiser and Wood [22], on the other hand, were performed in the presence of metallic Fe and are in good agreement.

Fig. 1b shows $RT\ln(K_D)$ for wadsleyite–magnesiowüstite experiments performed between 13 and 16 GPa at 1400°C. Previous experiments [19] are in good agreement with these results. Very little pressure dependence can be discerned, except for one point at 16 GPa that falls slightly below the other data. A least squares fit to all data between 13 and 14.5 GPa using Eq. 7, with the known activity composition relations of magnesiowüstite, yields values for W^{wad}_{FeMg} of 7.5 ± 1.2 kJ. A slightly different fitting procedure for determining activity–composition relations was outlined by Wiser and Wood [22] and uses the equations:

$$\log\gamma^{wad}_{Fe} = -X^{wad}_{Mg}\log Q + \int_0^{X^{wad}_{Mg}} \log Q \, dX^{wad}_{Mg} \quad (9)$$

$$\log\gamma^{wad}_{Mg} = (1-X^{wad}_{Mg})\log Q + \int_1^{X^{wad}_{Mg}} \log Q \, dX^{wad}_{Mg} \quad (10)$$

where

$$\log Q = \log\left[\frac{a^{Mw}_{Mg} X^{wad}_{Fe}}{a^{Mw}_{Fe} X^{wad}_{Mg}}\right] \quad (11)$$

Using this method W^{wad}_{FeMg} is calculated to be 8.6 ± 1.5 kJ between 13 and 14.5 GPa, which is consistent with the value of 7.5 kJ from the least squares fit of Eq. 7. There is no significant or systematic variation in the value of W^{wad}_{FeMg} obtained by fitting the data at each individual pressure. A symmetric solution model fits the experimental data very well and any degree of asymmetry must be much smaller than can be detected with these data. As shown in Table 4 this is the largest determined interaction parameter of the three $(Mg,Fe)_2SiO_4$ polymorphs.

Data for ringwoodite–magnesiowüstite Fe–Mg partitioning were refit along with previously published data [16] using Eq. 7 to give W^{ring}_{FeMg} = 4.1 ±

Table 4
Internally consistent thermodynamic data at 1400°C

	$G_{(1673K,1bar)}$ (J)	$V_{(1673K,1bar)}$ (J/bar)	$K_{(1673K,1bar)}$ (bar)	K'	Initial data
Mg_2SiO_4 Forsterite	−2 555 725	4.6053	957 000	4.6	[29]
Mg_2SiO_4 Wadsleyite	−2 514 481	4.2206	1 462 544	4.21	[29]
Mg_2SiO_4 Ringwoodite	−2 500 910	4.1484	1 453 028	4.4	[29]
MgO Periclase	−712 105	1.1932	1 259 000	4.1	[19]
$Mg_3Al_2Si_3O_{12}$ Pyrope	−7 379 204	11.8058	1 290 000	4	[30]
Fe_2SiO_4 Fayalite	−1 976 015	4.8494	998 484	4	[19]
Fe_2SiO_4 Wadsleyite	−1 955 055	4.4779	1 399 958	4	[19]
Fe_2SiO_4 Ringwoodite	−1 950 160	4.3813	1 607 810	5	[32]
FeO Wüstite	−443 151	1.2911	1 526 000	4	[19]
$Fe_3Al_2Si_3O_{12}$ Almandine	−6 514 529	12.1153	1 207 515	5.5	[31]
	W_U (J)	W_V (J/bar)			
Olivine	2 000	0.01			
Wadsleyite	7 500	0.0			
Ringwoodite	4 160	0.0			[16]
Magnesiowüstite	11 100	0.011			[21]
Garnet	0.0	0.0			[21]

All end-member data have been optimised from the initial data sources apart from data for periclase and wüstite and all values for K'. End-member data are reported as per mole of the indicated formula. Values for W_U and W_V are on a single site basis. The Gibbs free energy of each pure phase at P and T is calculated using the Murnaghan equation of state, i.e.: $G_{(T,P)} = G_{(T,1bar)} + V_{(T,1bar)}\{K_T/(K'-1)[(1+K'/K_T P)^{((K'-1)/K')}-1]\}$, where P is in bars. The partial molar free energy of (e.g.) the olivine Mg_2SiO_4 component would be $\overline{G}^{ol}_{Mg} = G^{ol}_{Mg(T,P)} + 2RT\ln X^{ol}_{Mg} + 2(Wu^{ol}_{FeMg} + PWv^{ol}_{FeMg})(1-X^{ol}_{Mg})^2$.

0.8 kJ/mol. This is within the error of the previously determined value [16]. One sample (V212) was made into a petrographic thin section for analysis with Fourier transform infrared spectroscopy. No bands corresponding to OH^- in either wadsleyite or ringwoodite were detected in this sample.

5. Thermodynamic model

In addition to using the partitioning data to refine activity–composition relations for the $(Mg,Fe)_2SiO_4$ polymorphs, by using Eq. 7 data can also be obtained on the Gibbs free energy change of the ion exchange reaction at pressure and temperature. Fitting partitioning data collected over a range of pressure at constant temperature also provides an estimate of the volume change of the ion exchange reaction at pressure and temperature. These thermodynamic properties provide very useful constraints with which to optimise internally consistent data for the end-member Mg_2SiO_4 and Fe_2SiO_4 polymorphs, which can then be used to construct an accurate phase diagram for this system at 1400°C. All high pressure and temperature constraints are extremely important because thermodynamic and elastic properties such as the heat capacity, expansivity and bulk modulus are known for most high-pressure phases only below 700°C, such that large extrapolations in temperature must be made to mantle conditions. In addition, phase equilibria data also lack the accuracy required to determine transformation intervals that may be below 0.2 GPa and must, therefore, be supported by a well-constrained thermodynamic model.

As a first step the volume, bulk modulus and Gibbs free energy of each end-member at 1 bar and 1400°C were calculated using existing thermodynamic data [19,27,29–32]. These data and the independently determined activity–composition relations were then used to calculate $RT\ln(K_D)$ for each experimental point at the particular pressure and composition using Eq. 7. In addition the end-member thermodynamic data were also

used to calculate the transformation pressures of the Mg_2SiO_4 forsterite to wadsleyite and wadsleyite to ringwoodite transitions and Fe_2SiO_4 fayalite to ringwoodite transition at 1400°C. Each experimental partitioning observation was compared with a calculated value and the difference in free energy was determined and weighted by the experimental uncertainty. Uncertainties in composition determined using the electron microprobe were used to weight the partitioning data and for end-member transforma- tions an uncertainty of 0.5 GPa was assumed. The calculated end-member phase transformations were compared with in situ experimental measurements [33–35]. The calculated and observed weighted differences were summed and this value was then minimised by adjusting the thermodynamic data for the end-member phases, except those for periclase and wüstite and values of K'. There are no measured thermodynamic or phase equilibria data on the fictive Fe_2SiO_4 wadsleyite end-member, so an additional constraint is required for this component. Determining the compositions of the three polymorphs at the point where they all coexist provides this constraint. At this 'triple point' the chemical potentials of each component must be equal in each phase. Fig. 2 shows a run product from an experiment (V254) where all three polymorphs were found to coexist. The olivine and wadsleyite compositions at the 'triple point' are 3–4% more Fe-rich compared to estimates from previous studies [10,27]. These compositions provide a crucial node on the phase diagram, which was missing from previous studies. The pressure of the triple point was allowed to vary in the optimisation but the resulting value (12.87 GPa) is consistent, within experimental error, with the pressure determined from the multianvil pressure calibration for this experiment (12.5 ± 0.5 GPa). A final constraint on the free energy of Fe_2SiO_4 wadsleyite is that it does not actually exist as a pure phase.

The optimised thermodynamic end-member data are reported in Table 4. The model reprodu-

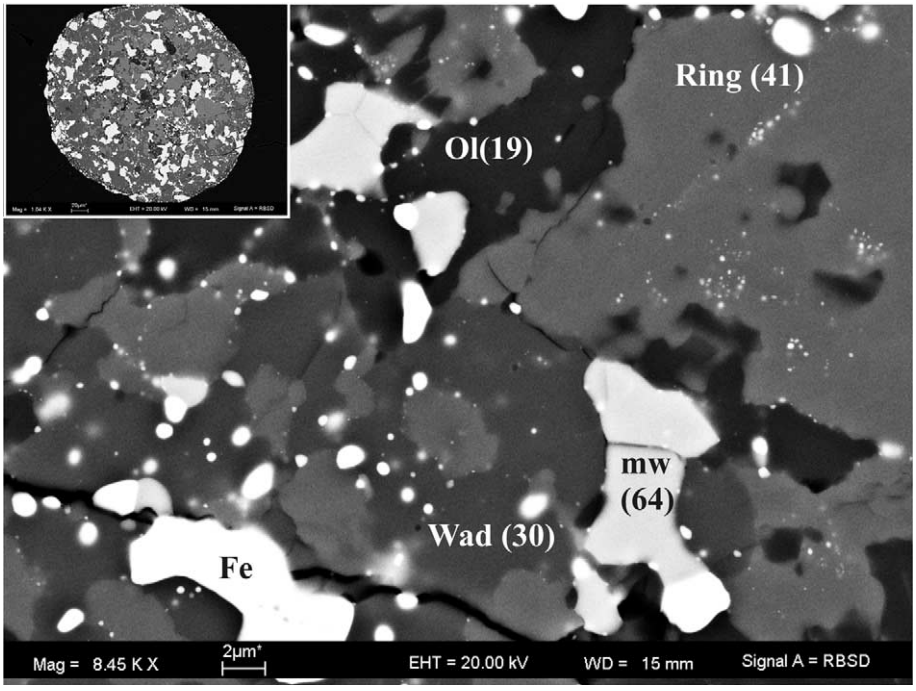

Fig. 2. Back-scattered electron image of coexisting olivine, wadsleyite and ringwoodite in sample V254. The Fe/(Fe+Mg)100 ratio of each phase is shown in brackets. The entire sample chamber is shown in the inset. Magnesiowüstite and metallic Fe are also scattered throughout the sample.

ces the experimentally determined end-member phase transformations to within 0.3 GPa and the maximum difference between calculated and observed $RT\ln(K_D)$ was 0.5 kJ/mol. In most cases the optimisation resulted in very minor changes from the initial thermodynamic data selected from previous studies. During the optimisation the largest change in the Gibbs free energy of any end-member was 0.4%. Changes in phase volumes as a result of the refinement were below 1% for all phases except that of Mg_2SiO_4 ringwoodite, which increased by 1.5% from the initial volume, calculated using the thermal expansion data of Suzuki et al. [36]. There is, however, a significant uncertainty resulting from the extrapolation of these data [36] to 1400°C because the measurements were made below 800°C. This is the case for all expansivities of the high-pressure phases. On the other hand, the thermal expansion of ringwoodite determined in a recent first-principles calculation [37] gives a volume at 1400°C that is in very good agreement with the optimised volume of Mg_2SiO_4 ringwoodite given in Table 4.

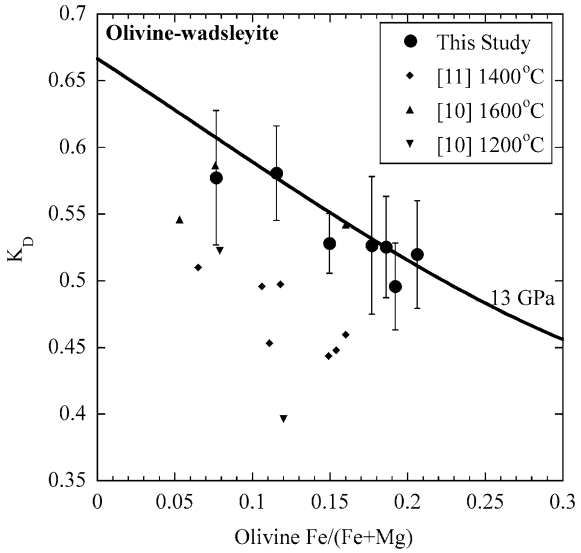

Fig. 3. The olivine–wadsleyite Fe–Mg distribution coefficient is calculated from the optimised thermodynamic model at 13 GPa (solid curve). $K_D = (X^{ol}_{Fe}X^{wad}_{Mg})/(X^{ol}_{Mg}X^{wad}_{Fe})$. Data points calculated from coexisting olivine and wadsleyite compositions at 1400°C that were also encountered in this study are shown (solid circles). These data were not used in the refinement but are in excellent agreement with the calculated curve. In general previous studies [10,11] have reported lower values of K_D.

6. Discussion

6.1. Evaluation of the thermodynamic model

The solid curve in Fig. 3 shows the olivine–wadsleyite Fe–Mg distribution coefficient K_D calculated from the optimised thermodynamic data at 13 GPa. In addition some partitioning data from coexisting olivine and wadsleyite, also observed in this study, are plotted. These data were not used in the optimisation, which was performed solely with data from partitioning involving magnesiowüstite. The calculated partitioning trend is, however, in excellent agreement with these experimental data. The calculated and observed K_D values reported here are generally higher than in previous studies, although data of Katsura and Ito [10] from 1600°C are quite close. The higher K_D values reflect a smaller difference in Fe contents between coexisting olivine and wadsleyite compared to the previous studies, which contributes to a narrower transformation pressure interval.

Fig. 4 shows the $(Mg,Fe)_2SiO_4$ phase diagram calculated from the thermodynamic data given in Table 4. Details of this calculation are given by Akaogi et al. [27]. The compositions of coexisting phases observed in this study are also shown, plotted at pressures determined using the multi-anvil pressure calibration. The coexisting compositions agree very well with those predicted by the model but the pressures are only accurate within the 0.5 GPa experimental uncertainty.

The optimised thermodynamic model can be used to calculate the pressure intervals of the $(Mg,Fe)_2SiO_4$ phase transformations for typical mantle compositions. The thermodynamic data are the best fit to the experimental observations but because values such as the volume and bulk modulus are correlated in the optimisation, a range of values can fit these data quite well. Numerous refinements showed, however, that as long as the model fits the experimental observations the calculated phase relations, and most impor-

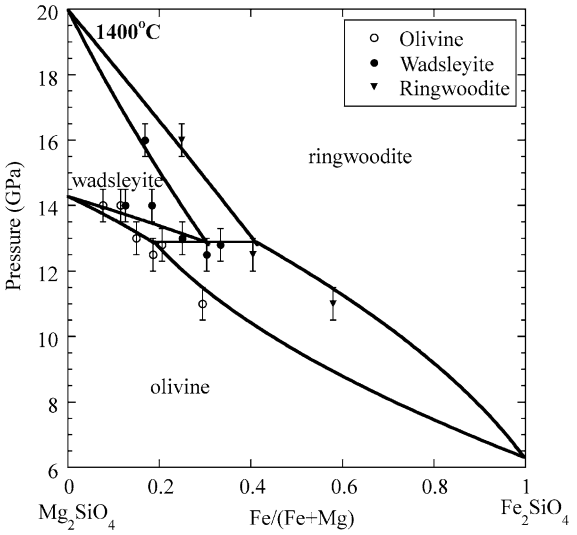

Fig. 4. Phase relations in the system Mg_2SiO_4–Fe_2SiO_4 calculated from the optimised thermodynamic data at 1400°C. Compositions of coexisting $(Mg,Fe)_2SiO_4$ polymorphs that were also encountered in this study are shown at pressures corresponding to the multianvil calibration. The vertical error bars correspond to the pressure uncertainty in the multianvil, which is estimated from the pressure calibration to be approximately 0.5 GPa. The coexisting compositions are in very good agreement with the calculated phase diagram but the calculated and observed pressures are consistent only within the experimental pressure uncertainties.

tantly the transformation pressure intervals, change very little. Another consequence of this, however, is that apart from the interaction parameters the optimised end-member data are only valid as part of this internally consistent data set.

Uncertainties in the model arise from the uncertainties in the interaction parameters, compositional variation in the analysed run products and in the end-member phase transformation pressure uncertainties. These uncertainties were used to weight the refinement, however, they can also be propagated through the refinement to determine limits of the model that still just fit the experimental uncertainties. These limits can be used to assess uncertainties on particular calculations. For the transformation interval of $(Mg_{0.9},Fe_{0.1})_2SiO_4$ olivine to wadsleyite, for example, the model predicts a pressure interval of 0.25 GPa, whilst alternative refinements that can still just fit within the errors on the experimental data predict this interval to be 0.4 GPa. This means that while the optimised fit to the experimental data yields a depth interval for the $(Mg_{0.9},Fe_{0.1})_2SiO_4$ transformation of 8 km, an interval of 12 km would still be just within the experimental uncertainties.

6.2. *Implications for the width of the 410 km discontinuity*

Estimates for the width of *d*410 vary between 4 and 35 km [38]. Although this range may to some degree be an artefact of the different seismological techniques employed, the range might also reflect real variations in the thickness caused by local differences in the chemical and physical properties of the transition zone. There are a number of potential factors, such as the presence of H_2O, which could cause the olivine to wadsleyite transformation to be quite broad. What is perhaps initially more intriguing, however, is to determine if there are conditions in the earth that can produce a very sharp transformation of olivine to wadsleyite over an interval of 4 km thick or less [8]. Specifically it is important to ascertain whether a sharp discontinuity is consistent with the generally accepted view that the mantle is dominantly of peridotite composition.

In Fig. 5a an enlargement of the calculated olivine to wadsleyite transformation is shown. For an $(Mg_{0.9},Fe_{0.1})_2SiO_4$ composition the transformation interval is calculated to be approximately 0.25 GPa, which would be equivalent to a depth interval at *d*410 of about 8 km. Katsura and Ito [10] determined this interval to be approximately 25 km wide at 1200°C and 14 km at 1600°C. These results, when interpolated, give a width of approximately 19 km at 1400°C. While the calculated interval at 1400°C is much narrower than determined in this previous experimental study, there is agreement when the pressure uncertainty in the study of Katsura and Ito is considered. It is also possible that factors such as the presence of H_2O or Fe^{3+} could have influenced the results of Katsura and Ito leading to a slightly broader transformation depth estimate.

Peridotite in the region of *d*410 would be comprised of approximately 60 mol% olivine, 30

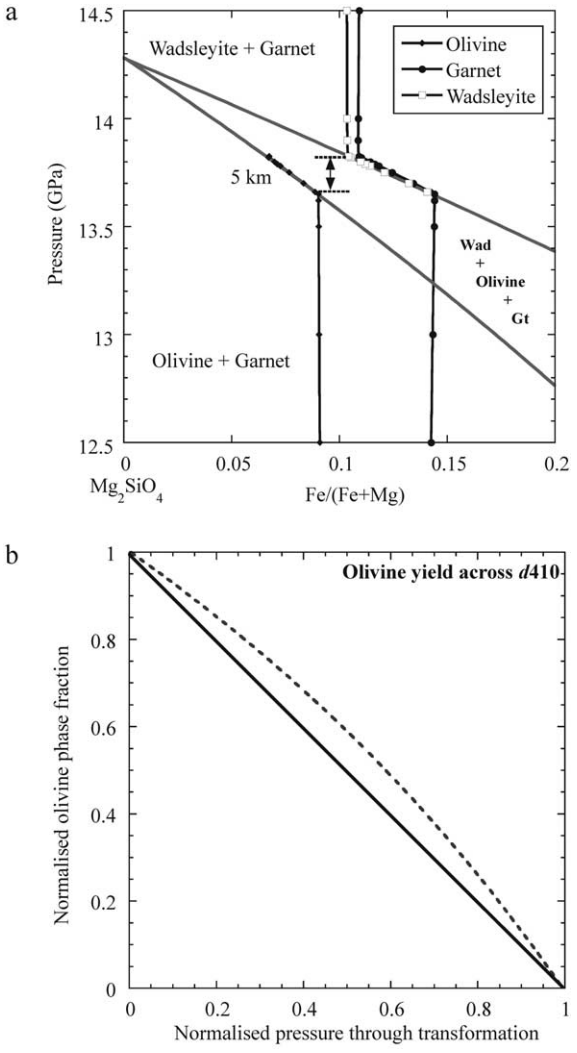

Fig. 5. (a) The olivine to wadsleyite transformation in the Mg_2SiO_4–Fe_2SiO_4 system calculated using the optimised thermodynamic data. The compositions of olivine, wadsleyite and garnet as they change across the transformation are indicated as calculated for a peridotite composition containing 60% $(Mg,Fe)_2SiO_4$ and 40% $(Mg,Fe)_3Al_2Si_3O_{12}$ with a bulk Fe/(Fe+Mg) ratio of 10.5%. The calculated width of *d*410 for this composition is indicated in km. The yield of olivine with increasing pressure across the transformation for this peridotite composition is shown as the dashed curve in panel b. The olivine content and the pressure have been normalised. The solid line is a linear transformation.

mol% majoritic garnet and 10 mol% clinopyroxene [14]. As a result of Fe–Mg partitioning between these minerals the Fe content of the $(Mg,Fe)_2SiO_4$ polymorph will not remain constant but will increase on transforming from olivine to wadsleyite [14,39]. In order to include this influence, which can effectively sharpen the discontinuity, previously reported Fe–Mg partitioning data between $(Mg,Fe)_3Al_2Si_3O_{12}$ garnet, olivine, magnesiowüstite and ringwoodite [21,24] were used to optimise internally consistent thermodynamic data for garnet Fe–Mg partitioning. These optimised thermodynamic data are also given in Table 4. Although garnet under transition zone conditions would be majoritic and Ca-bearing, previous work [21] has shown that these components have little combined effect on garnet Fe–Mg partitioning, probably because their individual effects are in opposite directions. Similarly in this analysis the presence of at least 10% clinopyroxene at the transformation conditions has been ignored. As the Fe content of clinopyroxene at these conditions will be lower than the other phases its potential to sharpen the transformation interval can only be smaller than a similar quantity of garnet.

Fig. 5a shows a calculation of the Fe/(Fe+Mg) ratios of olivine, wadsleyite and garnet as a function of depth for a peridotite composition containing 60% $(Mg,Fe)_2SiO_4$ and 40% $(Mg,Fe)_3Al_2Si_3O_{12}$ with a bulk Fe/(Fe+Mg) ratio of 0.105. The calculation was performed by minimising the free energy of the system at each pressure. For this composition the calculated transformation interval is approximately 5 km. In comparison to the transformation of monomineralic $(Mg_{0.9},Fe_{0.1})_2SiO_4$, in the presence of garnet the transformation is significantly sharpened as a result of the interphase Fe–Mg partitioning. Olivine is Fe-poor on the low-pressure side of the transformation in comparison to wadsleyite on the high-pressure side because Fe partitions less favourably into garnet in the wadsleyite stability field than in the olivine field. The transformation therefore starts at a higher pressure and is complete at a lower pressure than in the monomineralic case. This effect sharpens the transformation interval by approximately 35%.

Before we can apply this discontinuity width to seismic observations, however, there are still a number of further factors to be considered. Gudfinnsson and Wood [40] investigated the influence

of various minor elements on the olivine to wadsleyite transformation interval. They found that the preferential partitioning of Al, Ti and Cr into wadsleyite would broaden the transformation by 1–2 km. This influence must be added to the width determined in Fig. 5a as such minor elements were not included in the calculation. This does not include the effect of H_2O, which will be addressed later. Several studies have raised the possibility that strong curvature in the boundaries of the two-phase region would result in mineral transformation yields that were a strong non-linear function of pressure and that this could make the transition appear sharper in seismic observations [12,13]. In Fig. 5b the olivine yield across the transformation is plotted from the calculation on a peridotite composition shown in Fig. 5a. The yield is almost linear and a comparison with the results of Helffrich and Wood [13] implies that the observed seismic reflection would not appear significantly sharper than the actual transition interval. Another possibility is that focusing effects as a result of topography on *d*410 could make the seismically observed transformation appear sharper in isolated observations [38]. Repeated observations from a number of earthquakes are the only way to clarify this point.

In adiabatically convecting mantle the temperature change resulting from the latent heat of the transition will result in a broader transformation interval in comparison to the isothermal case shown in Fig. 5a. The temperature change of the olivine to wadsleyite transformation can be estimated from the relation [41]:

$$\Delta T \approx -T\frac{\mathrm{d}P}{\mathrm{d}T}\Delta V/C_\mathrm{p} \qquad (12)$$

where ΔV is the volume change of the transformation and C_p is the heat capacity. Taking the volume change from the current refinement, and previous estimates for C_p and the Clapeyron slope [27,33] the temperature change in a peridotite composition is calculated to be approximately 50°, which given the uncertainties in this calculation would broaden the discontinuity by between 5 and 7 km. This would make a total thickness for *d*410 of approximately 10 km. If the vertical component of mantle flow is lower than approximately 1 mm/yr, however, then thermal conductivity over a 10 km depth becomes more rapid than convection [42,43]. In this case the temperature change across the discontinuity would be smeared out over a greater depth and the temperature drop and resulting broadening at the discontinuity due to latent heat would be reduced. For vertical flow rates of less than 0.1 mm/yr the temperature change across the discontinuity would be smeared out to such an extent that it would have a minor effect on the discontinuity width, which would therefore return to approximately 6 km. It seems quite possible that significant regions of the mantle, that are far away from mantle plumes and subduction zones, have relatively small vertical flow velocities. If estimates of less than 6 km for the thickness of *d*410 are correct [7–9] then these regions of the mantle must have suitably slow vertical flow rates if they are composed of typical mantle peridotite.

Considering the aforementioned factors, the olivine–wadsleyite transformation interval at 1400°C in dry peridotite with low or no vertical component of mantle flow would be approximately 6 km thick. This width is in excellent agreement with some previous experimental and thermodynamic estimates [14,44] although the exact reasoning behind these previous estimates differs somewhat from this study. 6 km is at the narrow end of the range of seismic estimates for the width of *d*410, which go from 4 to 35 km [38]. It is not clear just how precise these seismic estimates are, or if focusing effects may be responsible for some of the very sharp observations. If, however, we take the simplifying assumption that this variation reflects real differences in the mantle between different regions, then it is important to consider possible factors that might cause *d*410 to be either sharper or broader than 6 km in various parts of the mantle. It should be noted that the experimental data used in this study would also be consistent with a transformation interval both sharper than 6 km and as wide as 10 km when all uncertainties are considered.

Considering first factors that could further sharpen the transformation. The results of Katsura and Ito [10] imply that increasing the temperature by 100° would sharpen the olivine to wads-

leyite transformation by approximately 3 km. Temperatures at *d*410 between 1450 and 1500°C could, therefore, result in a transformation interval below 4 km. An increase in the garnet content of the mantle would also sharpen the transformation. I calculate that increasing the garnet content from 40 to 50% decreases the width by approximately 1 km. Similarly, if the Fe/(Fe+Mg) ratio of the mantle were lower by 1% this would also sharpen the transformation by approximately 1 km. A potential cause of this would be if the oxygen fugacity in the transition zone is low enough for a metallic Ni–Fe alloy to precipitate, as has been proposed in several studies [20,45]. This would lower the Fe/(Fe+Mg) ratio of silicate minerals in the transition zone region.

There are several effects that could make the transformation at *d*410 broader than 6 km. Obviously we would expect broader transformations in colder, garnet-poor or FeO-rich regions of the mantle. The transformation would also be broadened by 5–7 km in mantle with a high vertical component of mantle flow. The solubility of H_2O in the mantle phases, however, has perhaps the most dramatic potential to broaden the discontinuity. Wood [15] first proposed that the high partition coefficient of OH^- between wadsleyite and olivine means that relatively low OH^- concentrations would cause a significant broadening of the *d*410 transformation. This has been to some extent experimentally confirmed [46]. The model of Wood predicts that the addition of even 100 ppm H_2O would broaden the discontinuity by approximately 3 km. Therefore to produce a discontinuity of 6 km or less it is difficult to envisage a mantle that is anything other than exceedingly dry in this region ($H_2O < 100$ ppm). Subduction of H_2O-rich material and mobility of H_2O-rich fluids and melts may result, however, in a heterogeneous mantle H_2O distribution. Recent observations that *d*410 is between 20 and 30 km thick beneath some parts of the Mediterranean [5] may be evidence for higher mantle H_2O contents in these regions. If the transformation is 6 km thick in dry mantle then a 20 km wide discontinuity would suggest a mantle H_2O content of approximately 500 ppm using the model of Wood [15]. It is important to note that the model of Wood predicts the transformation to become increasingly non-linear with increasing H_2O concentration. For high H_2O contents the seismically observed discontinuity may therefore appear sharper than the actual transformation thickness. Seismic observations that fit well to a non-linear transformation at *d*410 [18,47] might also therefore be an indicator for the presence of H_2O in the mantle because the dry transformation would be linear.

6.3. Implications for the width of the 520 km discontinuity

Fig. 6a shows the wadsleyite to ringwoodite transformation for the same peridotite composition as shown in Fig. 5a. The calculated monomineralic wadsleyite transformation is about 0.9 GPa for a Fe/(Fe+Mg) ratio of 0.1. This is consistent with the width determined by Katsura and Ito [15] at 1200 and 1600°C. As H_2O and Fe^{3+} have similar solubilities in both wadsleyite and ringwoodite [48,49] these components are likely to have a relatively small influence on the width of this transformation. The presence of garnet in the mantle will reduce the transformation interval to approximately 0.7 GPa, which would be equivalent to a depth interval of 20 km. The yield of this transformation is also relatively linear as shown in Fig. 6b. Several seismological studies employing long-period S-wave observations (SS precursors or ScS reverberations) have identified reflections from a discontinuity at around 520 km [50–52]. The absence of reflections at 520 km in high-frequency studies [8] has been used to propose a thickness of between 10 and 50 km [38,47] for this discontinuity. The phase transformation of wadsleyite to ringwoodite in peridotite mantle would, therefore, have a width quite consistent with these seismic observations.

7. Conclusions

Fe–Mg partitioning between magnesiowüstite and the $(Mg,Fe)_2SiO_4$ polymorphs collected over a range of pressure at 1400°C has been used to refine thermodynamic data for these phases and calculate phase diagrams for the olivine to wads-

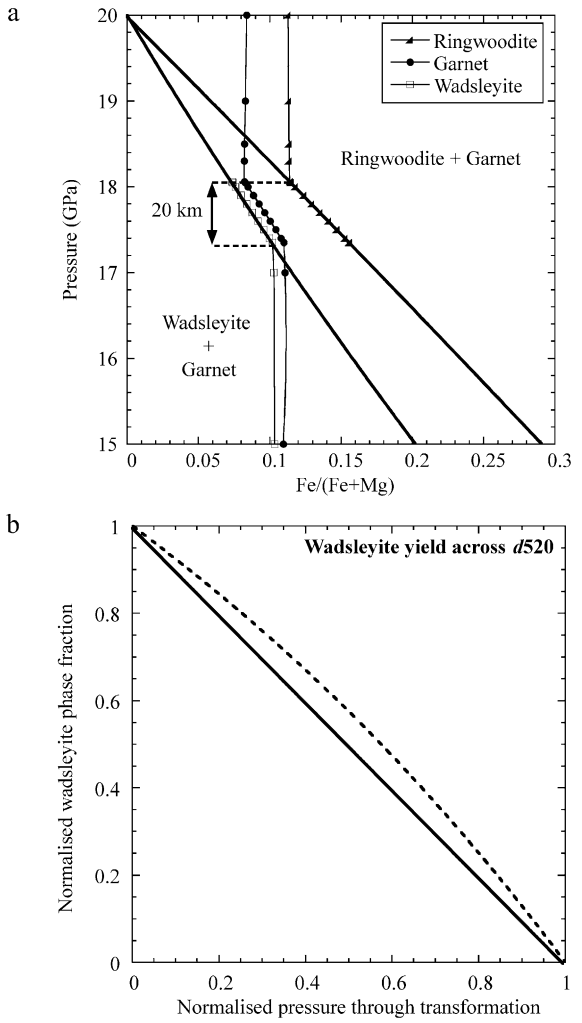

Fig. 6. (a) The wadsleyite to ringwoodite transformation calculated using the optimised thermodynamic data. The compositions of wadsleyite, ringwoodite and garnet have been calculated for the same peridotite composition as shown in Fig. 5. The calculated width of *d*520 for this composition is indicated in km. The yield of wadsleyite with increasing pressure across the transformation for this composition is shown as the dashed curve in panel b.

leyite and wadsleyite to ringwoodite transformations.

Using previously published activity–composition relations for magnesiowüstite the following symmetric Margules interaction parameters for single sites have been determined: $W_{\mathrm{FeMg}}^{\mathrm{wadsleyite}} = 7.5\ (1.2)$ kJ/mol; $W_{\mathrm{FeMg}}^{\mathrm{ringwoodite}} = 4.1\ (0.8)$ kJ/mol; $W_{\mathrm{FeMg}}^{\mathrm{olivine}} = 2.0\ (1.0)$ kJ/mol.

The non-ideality of Fe–Mg mixing in wadsleyite appears to be significantly greater than in the other two polymorphs.

The calculated olivine to wadsleyite transformation pressure interval is narrower than previous determinations. This can be attributed to a smaller difference in Fe contents between coexisting olivine and wadsleyite calculated and observed in this study. A potential cause of this may have been the use of metallic Fe, which lowered the ferric iron contents particularly in wadsleyite in these partitioning experiments. Such lower oxygen fugacities are, however, likely to be more applicable to the Earth's transition zone.

Using published data on the Fe–Mg partitioning between garnet and the $(Mg,Fe)_2SiO_4$ polymorphs the olivine to wadsleyite transformation interval was calculated to be approximately 0.2 GPa or equivalent to 6 km for a typical dry mantle peridotite composition at 1400°C. Across the transformation the yield was found to vary almost linearly with pressure.

Higher temperatures would sharpen the olivine to wadsleyite transformation such that widths below 6 km are plausible at mantle temperatures of 1500°C. Increasing the peridotite garnet content by 10% or lowering the bulk Fe/(Fe+Mg) ratio by 1% would sharpen the transformation by approximately 1 km.

In mantle with a high-velocity vertical component of mantle flow the latent heat change resulting from the transformation would cause a broadening of the olivine to wadsleyite transition by 5–7 km. In regions with low or no vertical mantle flow component thermal conductivity will counteract this broadening effect and the transformation will remain sharp. The presence of H_2O in the mantle is likely to make the transformation broader and increasingly non-linear. Estimates on the order of 20 km for the width of *d*410 from some seismic observations [5] could result from approximately 500 ppm of H_2O in the mantle.

The wadsleyite to ringwoodite transformation in a dry peridotite composition at 1400°C is estimated to be approximately 20 km thick, which is in good agreement with previous estimates. The yield of this transformation is also very close to

linear. The presence of H_2O or Fe^{3+} is not expected to significantly influence the position or width of this transformation.

Acknowledgements

I would like to thank G. Herrmannsdörfer, H. Fischer, H. Schultz, A. Markert and D. Krauße for their technical assistance. Discussions with S. van der Lee, T. Katsura, F. Marton and J. Ganguly greatly improved the manuscript, as did constructive reviews from G. Helffrich and Y. Fei. *[BW]*

References

[1] C.B. Agee, Phase transformations and seismic structure in the upper mantle and transition zone, in: R.J. Hemley, D. Mao (Eds.), Ultrahigh-Pressure Mineralogy, Rev. Mineral. 37 (1999) 343–367.
[2] D.J. Weidner, Y. Wang, Phase transformations: implications for mantle structure, in: S. Karato, A.M. Forte, R.C. Liebermann, G. Masters, L. Stixrude (Eds.), Earth's Deep Interior: Mineral Physics and Tomography From the Atomic to the Global Scale, Geophys. Monogr. 117 (2000) 215–235.
[3] J. Revenaugh, T.H. Jordan, A study of mantle layering beneath the western Pacific, J. Geophys. Res. 94 (1989) 5787–5813.
[4] Y. Gu, A.M. Dziewonski, C.B. Agee, Global de-correlation of the topography of transition zone discontinuities, Earth Planet. Sci. Lett. 157 (1998) 57–67.
[5] M. van der Meijde, F. Marone, D. Giardini, S. van der Lee, Seismological evidence for water deep in Earth's upper mantle, Science 300 (2003) 1556–1558.
[6] F. Xu, J.E. Vidale, P.S. Earle, H.M. Benz, Mantle discontinuities under southern Africa from precursors to $P'P'_{df}$, Geophys. Res. Lett. 25 (1998) 571–574.
[7] A. Yamazaki, K. Hirahara, The thickness of upper mantle discontinuities, as inferred from short-period J-Array data, Geophys. Res. Lett. 21 (1994) 1811–1814.
[8] H.M. Benz, J.E. Vidale, Sharpness of upper-mantle discontinuities determined from high-frequency reflections, Nature 365 (1993) 147–150.
[9] S. Rost, M. Weber, The upper mantle transition zone discontinuities in the Pacific as determined by short-period array data, Earth Planet. Sci Lett. 204 (2002) 347–361.
[10] T. Katsura, E. Ito, The system Mg_2SiO_4-Fe_2SiO_4 at high pressure and temperature: precise determination of stabilities of olivine, modified spinel and spinel, J. Geophys. Res. 94 (1989) 15663–15670.
[11] Y. Fei, C.M. Bertka, Phase transformations in the Earth's mantle and mantle mineralogy, in: Y. Fei, C.M. Bertka, B.O. Mysen (Eds.), Mantle Petrology: Field Observations and High Pressure Experimentation, vol. 6, The Geochemical Society, Washington, DC, 1999, pp. 189–207.
[12] L. Stixrude, Structure and sharpness of phase transitions and mantle discontinuities, J. Geophys. Res. 102 (1997) 14835–14852.
[13] G.R. Helffrich, B.J. Wood, 410 km discontinuity sharpness and the form of the olivine phase diagram: resolution of apparent seismic contradictions, Geophys. J. Int. 126 (1996) 7–12.
[14] T. Irifune, M. Isshiki, Iron partitioning in a pyrolite mantle and the nature of the 410-km seismic discontinuity, Nature 349 (1998) 409–411.
[15] B.J. Wood, The effect of H_2O on the 410-kilometer seismic discontinuity, Science 268 (1995) 74–76.
[16] D.J. Frost, F. Langenhorst, P.A. van Aken, Fe–Mg partitioning between ringwoodite and magnesiowüstite and the effect of pressure, temperature and oxygen fugacity, Phys. Chem. Miner. 28 (2001) 455–470.
[17] A.B. Woodland, R.J. Angel, Phase relations in the system fayalite-magnetite at high pressures and temperatures, Contrib. Mineral. Petrol. 139 (2000) 734–747.
[18] T. Melbourne, D. Helmberger, Fine structure of the 410-km discontinuity, J. Geophys. Res. 103 (1998) 10091–10102.
[19] Y. Fei, H.K. Mao, B.O. Mysen, Experimental element partitioning and calculation of phase relations in the MgO–FeO–SiO_2 system at high pressure and high temperature, J. Geophys. Res. 96 (1991) 2157–2169.
[20] H.St.C. O'Neill, D.C. Rubie, D. Canil, C.A. Geiger, C.R. Ross, F. Seifert, A.B. Woodland, Ferric iron in the upper mantle and in transition zone assemblages: implications for relative oxygen fugacities in the mantle, Geophys. Monogr. 74 (IUGG 14) (1993) 73–89.
[21] D.J. Frost, Fe^{2+}–Mg partitioning between garnet, magnesiowüstite and $(Mg,Fe)_2SiO_4$ phases of the transition zone, Am. Mineral. 88 (2003) 387–397.
[22] N. Wiser, B.J. Wood, Experimental determination of activities in Fe–Mg olivine at 1400K, Contrib. Mineral. Petrol. 108 (1991) 146–153.
[23] H.St.C. O'Neill, M.I. Pownceby, C.A. McCammon, The magnesiowüstite-iron equilibrium and its implications for the activity-composition relations of $(Mg,Fe)_2SiO_4$ olivine solid solutions, Contrib. Mineral. Petrol. (2003) in press.
[24] H.St.C. O'Neill, B.J. Wood, An experimental study of Fe–Mg partitioning between garnet and olivine and its calibration as a geothermometer, Contrib. Mineral. Petrol. 70 (1979) 59–70.
[25] I. Srečec, A. Ender, E. Woermann, W. Gans, E. Jacobsson, G. Eriksson, E. Rosén, Activity–composition relations of the magnesiowüstite solid solution series in equilibrium with metallic iron in the temperature range 1050–1400K, Phys. Chem. Miner. 14 (1987) 492–498.
[26] G.W. Fisher, L.G. Medaris, Cell dimensions and x-ray determinative curve for synthetic Mg–Fe olivines, Am. Mineral. 54 (1969) 741–753.

[27] M. Akaogi, E. Ito, A. Navrotsky, Olivine-modified spinel-spinel transitions in the system Mg_2SiO_4-Fe_2SiO_4: calorimetric measurements, thermochemical calculation, and geophysical application, J. Geophys. Res. 94 (1989) 15671–15685.

[28] C. McCammon, Effect of pressure on the composition of the lower mantle end member Fe_xO, Science 259 (1993) 66–68.

[29] M.H.G. Jacobs, H.A.J. Oonk, The Gibbs energy formulation of the α, β, and γ forms of Mg_2SiO_4 using Grover, Getting and Kennedy's empirical relation between volume and bulk modulus, Phys. Chem. Miner. 28 (2001) 572–585.

[30] M. Akaogi, A. Tanaka, E. Ito, Garnet–ilmenite–perovskite transitions in the system $Mg_4Si_4O_{12}$–$Mg_3Al_2Si_3O_{12}$ at high pressures and high temperatures: phase equilibria, calorimetry and implications for mantle structure, Phys. Earth Planet. Inter. 132 (2002) 303–324.

[31] M. Akaogi, N. Ohmura, T. Suzuki, High-pressure dissociation of $Fe_3Al_2Si_3O_{12}$ garnet: phase boundary determined by phase equilibrium experiments and calorimetry, Phys. Earth Planet. Inter. 106 (1998) 103–113.

[32] K. Matsuzaka, M. Akaogi, T. Suzuki, T. Suda, Mg–Fe partitioning between silicate spinel and magnesiowüstite at high pressures: experimental determination and calculation of phase relations in the system Mg_2SiO_4-Fe_2SiO_4, Phys. Chem. Miner. 27 (2000) 310–319.

[33] H. Morishima, T. Kato, M. Suto, E. Ohtani, S. Urakawa, W. Utsumi, O. Shimomura, T. Kikegawa, The phase boundary between α and β Mg_2SiO_4 determined by in situ X-ray observation, Science 265 (1994) 1202–1203.

[34] A. Suzuki, E. Ohtani, H. Morishima, T. Kubo, Y. Kanbe, T. Kondo, In situ determination of the phase boundary between wadsleyite and ringwoodite in Mg_2SiO_4, Geophys. Res. Lett. 27 (2000) 803–806.

[35] T. Yagi, M. Akaogi, O. Shimomura, T. Suzuki, S. Akimoto, In situ observation of the olivine–spinel phase transition in Fe_2SiO_4 using synchrotron radiation, J. Geophys. Res. (1987) 6207–6213.

[36] I. Suzuki, E. Ohtani, M. Kumazawa, Thermal expansion of γ-Mg_2SiO_4, J. Phys. Earth 27 (1979) 53–61.

[37] P. Piekarz, P.T. Jochym, K. Parlinski, J. Lazewski, High-pressure and thermal properties of γ-Mg_2SiO_4 from first-principles calculations, J. Chem. Phys. 117 (2002) 3340–3344.

[38] P.M. Shearer, Upper mantle seismic discontinuities, in: S. Karato, A.M. Forte, R.C. Liebermann, G. Masters, L. Stixrude (Eds.), Earth's Deep Interior: Mineral Physics and Tomography From the Atomic to the Global Scale, Geophys. Monogr. 117 (2000) 115–131.

[39] M. Akaogi, S. Akimoto, High-pressure phase equilibria in a garnet lherzolite, with special reference to Mg^{2+}–Fe^{2+} partitioning among constituent minerals, Phys. Earth Planet. Inter. 19 (1979) 31–51.

[40] G.H. Gudfinnsson, B.J. Wood, The effect of trace elements on the olivine–wadsleyite transformation, Am. Mineral. 83 (1998) 1037–1044.

[41] T. Katsura, E. Ito, Temperature of the transition zone, Geophys. Res. Lett. 16 (1989) 425–428.

[42] R. Jeanloz, A.B. Thompson, Phase transitions and mantle discontinuities, Rev. Geophys. Space Phys. 21 (1983) 51–74.

[43] Y. Xu, T.J. Shankland, S. Linhardt, D.C. Rubie, F. Langenhorst, K. Klasinski, Thermal diffusivity and conductivity measurements of olivine, wadsleyite and ringwoodite to 20 GPa and 1373 K, Phys. Earth Planet. Inter. (in press).

[44] C.R. Bina, B.J. Wood, Olivine-spinel transitions: experimental and thermodynamic constraints and implications for the nature of the 400-km seismic discontinuity, J. Geophys. Res. 92 (1987) 4853–4866.

[45] C. Ballhaus, Is the upper mantle metal-saturated?, Earth Planet. Sci. Lett. 132 (1995) 75–86.

[46] J.R. Smyth, D.J. Frost, The effect of water on the 410-km discontinuity: an experimental study, Geophys. Res. Lett. 29 (2002) 10.1029/2001GL014418.

[47] F. Neele, Sharp 400-km discontinuity from short-period P reflections, Geophys. Res. Lett. 23 (1996) 419–422.

[48] D.L. Kohlstedt, H. Keppler, D.C. Rubie, Solubility of water in the α, β and γ phases of $(Mg,Fe)_2SiO_4$, Contrib. Mineral. Petrol. 123 (1996) 345–357.

[49] H.St.C. O'Neill, C.A. McCammon, D. Canil, D.C. Rubie, C.R. Ross, F. Seifert, Mössbauer spectroscopy of mantle transition zone phases and determination of minimum Fe^{3+} content, Am. Mineral. 78 (1993) 456–460.

[50] J. Revenaugh, T.H. Jordan, Mantle layering from ScS reverberations 2. The transition zone, J. Geophys. Res. 96 (1991) 19763–19780.

[51] P.M. Shearer, Transition zone velocity gradients and the 520-km discontinuity, J. Geophys. Res. 101 (1996) 3053–3066.

[52] M.P. Flanagan, P.M. Shearer, Global mapping of topography on the transition zone velocity discontinuities by stacking *SS* precursors, J. Geophys. Res. 103 (1998) 2673–2702.